

# Synthesis and thermal characterization of NZP compounds $\text{Na}_{1-x}\text{Li}_x\text{Zr}_2(\text{PO}_4)_3$ ( $x = 0.00\text{--}0.75$ )

U. Ahmadu · A. O. Musa · S. A. Jonah ·  
N. Rabiu

Received: 18 June 2009 / Accepted: 7 January 2010 / Published online: 28 January 2010  
© Akadémiai Kiadó, Budapest, Hungary 2010

**Abstract** Sodium zirconium phosphate (NZP) composition  $\text{Na}_{1-x}\text{Li}_x\text{Zr}_2(\text{PO}_4)_3$ ,  $x = 0.00\text{--}0.75$  has been synthesized by method of solid state reaction method from  $\text{Na}_2\text{CO}_3 \cdot \text{H}_2\text{O}$ ,  $\text{Li}_2\text{CO}_3$ ,  $\text{ZrO}_2$ , and  $\text{NH}_4\text{H}_2\text{PO}_4$ , sintering at 1050–1250 °C for 8 h only in other to determine the effect on thermal properties, such as the phase formation of the compound. The materials have been characterized by TGA and DTA thermal analysis methods from room temperature to 1000 °C. It was observed that the increase in lithium content of the samples increased thermal stability of the samples and the DTA peaks shifted towards higher temperatures with increase in lithium content. The thermal stability regions for all the sample was observed to be from 640 °C. The sample with the highest lithium content,  $x = 0.75$ , exhibited the greatest thermal stability over the temperature range.

**Keywords** Thermal analysis · Sodium zirconium phosphate · NASICON

## Introduction

One of the most important materials that is being presently studied in materials science is sodium zirconium phosphate,  $\text{NaZr}_2(\text{PO}_4)_3$ , otherwise popularly known as NASICON or NZP. The material has been found to have very unique properties such as being the only substance that can accommodate atoms of different sizes in its various lattice sites [1]. The Na, Zr, and phosphorus can all be substituted, except oxygen, resulting in compositions with varying physical and chemical properties suitable for diverse applications. Several studies have been undertaken reflecting the various potential applications such as its use as substrate material for oxide-coating [1, 2], for immobilization of nuclear wastes [3], applications in near zero, or negative thermal expansion materials, in particular the relationship between the crystal structure of the compounds and their use to explain the processes underlying the thermal properties [4] and as electrode for rechargeable lithium battery applications [5] and gas sensors, among others.

We are carrying out series of characterizations, beginning with thermal analysis of lithium-substituted composition  $\text{Na}_{1-x}\text{Li}_x\text{Zr}_2(\text{PO}_4)_3$  ( $x = 0.00\text{--}0.75$ ), with the intent of determining their suitability for applications as electrolytes for energy applications. Many studies have been carried out on NZP materials that were synthesized through various routes in other to obtain materials of good thermal and electrical characteristics, in particular by appropriate configuration of the sintering times and temperatures. This has ultimately led to the synthesis of pure phase and good crystalline materials with enhanced properties. Studies have shown, for example, that the minimum sintering temperature required for the formation of NASICON is about 1100 °C [6] at different sintering

U. Ahmadu (✉)  
Department of Physics, Federal University of Technology,  
Minna, Nigeria  
e-mail: u.ahmadu@yahoo.com

A. O. Musa  
Department of Physics, Bayero University, Kano, Nigeria

S. A. Jonah  
Centre for Energy Research and Training (CERT), Ahmadu  
Bello University, Zaria, Nigeria

N. Rabiu  
Department of Physics, Ahmadu Bello University, Zaria, Nigeria

times which may be as low as possible, but generally varying from 16 h [7] to as much as 20 h [8], aside from other intermediate and higher values. Kang and Cho [9], for example, in their study of two different formulations of NASICON compositions, have examined the balance between these two factors on the formation of the phases of the NASICON compound and found that there is indeed a particular balance that exists between them for the formation of NASICON to ensue. This study is therefore expected to elucidate this further. We have used a sintering time of only 8 h for both the sintering and other preliminary steps in the solid-state synthesis of the materials, making the aggregate time to be much less than had hitherto been reported in literature. We wish to determine whether NASICON could be formed within this period at a sintering temperature 1050–1250 °C. Thus, we studied four compositions and thermally examined their stability with respect to increasing lithium content between room temperature and 1000 °C using DTA and TG thermal analysis methods. Here, we report the results of the thermal characterization while the ongoing research on XRD, among others, is taking place to determine the phases and other relevant parameters relating to the materials.

## Experimental

### Synthesis

The preparation of these samples was carried out at the Centre for Energy Research and Development (CERD), O.A.U. Ile-Ife. Basic starting materials of analytical grade (>99%) were used, that is,  $\text{Na}_2\text{CO}_3 \cdot \text{H}_2\text{O}$ ,  $\text{ZrO}_2$ ,  $\text{Li}_2\text{CO}_3$ , and  $\text{NH}_4\text{H}_2\text{PO}_4$ . Stoichiometric amounts of these materials were mixed and thoroughly ground in an agate mortar for about 5 h in each case. The sample was then dried in air for about 4 h. Acetone was added in appropriate quantity to homogenize the mixture. Pellets of discs of 13 mm diameter and 6 mm thickness were prepared for sintering purposes under the pressure of  $7.42 \times 10^6 \text{ N/m}^2$ . The sintering was carried out at the National Metallurgical Development Centre (NMDC), Jos. All the samples were placed inside a gas-heated furnace for 8 h at successive temperatures 200, 500, 1050, 1100, 1150, 1200, and 1250 °C, respectively. Between each temperature, the samples were allowed to furnace cool to room temperature and the samples were thoroughly ground, re-mixed, pelletized, and placed back into the furnace for the next round of heating. The first two temperatures are to allow for the volatilization of by-products, ammonia, water and carbon dioxide. The other temperatures are for sintering to allow for the systematic study of the formation temperature of the

NZP and provide for regrinding to improve homogeneity, since a uniform heat treatment time of only 8 h was used. The maximum sintering temperature was 1250 °C.

### Thermal characterization

Specimens of the virgin powder samples were used for the measurement on DTA machine NETZCHDTA404PC in air, at the Centre for Energy Research and Development (CERD), O.A.U. Ile-Ife. The readings were taken between room temperature and 1000 °C at a heating rate of 20.0 K/min. The results are shown in Figs. 1, 2, 3, and 4. The TG was performed on virgin powder specimens from room temperature to about 1000 °C on an TG Shimadzu DT-30 thermal analyser in air at a heating rate of 20.0 K/min at the

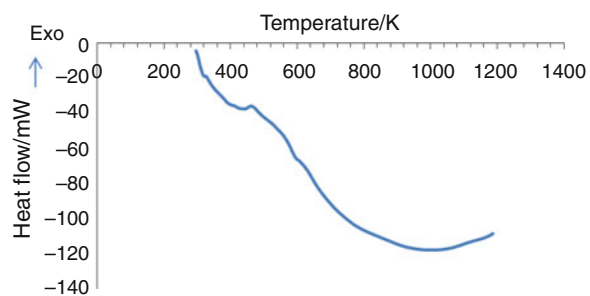


**Fig. 1** DTA plot of sample  $x = 0.00$  showing the exothermic peak at 188.9 °C

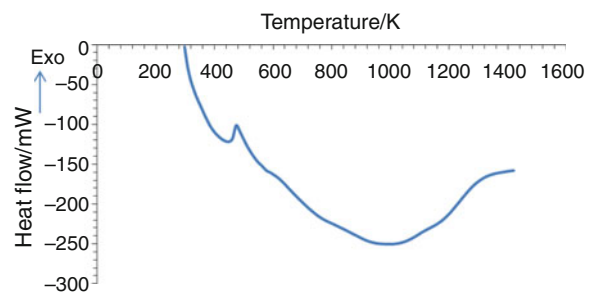


**Fig. 2** DTA plot of sample  $x = 0.25$  showing the exothermic peak at 200.0 °C

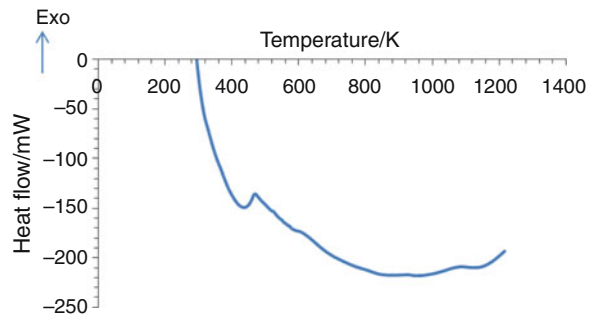


**Fig. 3** DTA plot of sample  $x = 0.50$  showing the exothermic peak at 196.4 °C

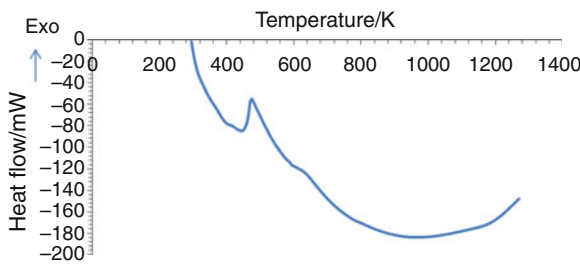


**Fig. 4** DTA plot of sample  $x = 0.75$  showing the exothermic peak at 201.7 °C

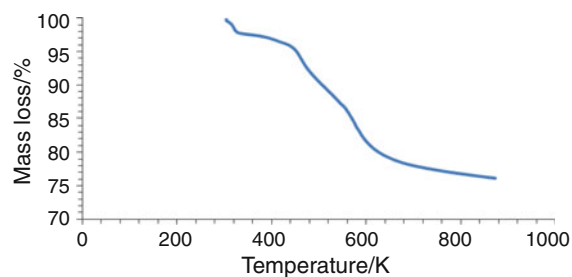


**Fig. 8** TG Plot of sample  $x = 0.75$  showing the four temperature regions of mass losses

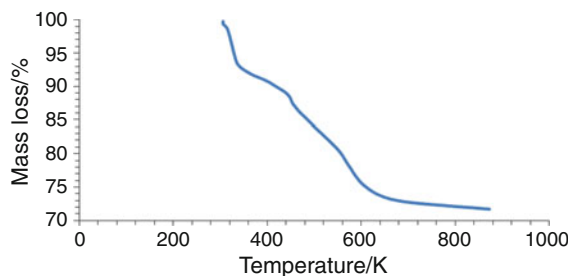


**Fig. 5** TG Plot of sample  $x = 0.00$  showing the four temperature regions of mass losses

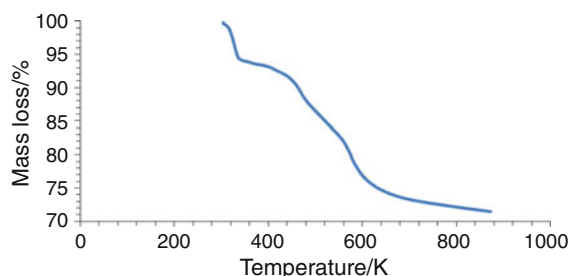


**Fig. 6** TG Plot of sample  $x = 0.25$  showing the four temperature regions of mass losses

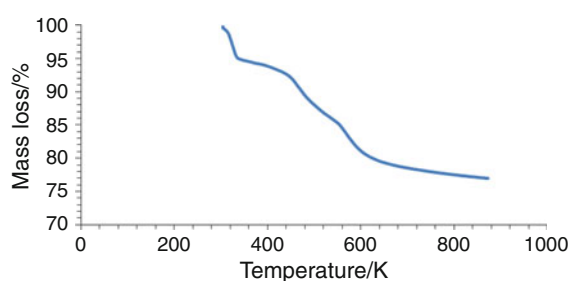


**Fig. 7** TG Plot of sample  $x = 0.50$  showing the four temperature regions of mass losses

University of Witwatersrand, South Africa. The plot of mass loss (%) versus temperature (K) of the samples is shown in Figs. 5, 6, 7, and 8.

## Results and discussions

For the sample  $x = 0.00$ , there is only one exothermic peak at 188.9 °C which began from 140 to 220 °C in the DTA plot. This can be attributed to the loss of water and water of hydration. The absorbed heat continued to increase until it reached a plateau between 680 and 760 °C, showing synthesis completion. This shows that the sample is stable in this region (Fig. 1), and is confirmed by the TG plot in Fig. 5, where the sample showed stability from 600 to 1000 °C.

Similar work by Naik et al. [10] on the sample, for example, has about eight peaks in the DTA plots, three are endothermic and the rest are exothermic. They attributed the endothermic (largest) peak which they found at 120 °C to the elimination of water from the mixture. The work by Petkov et al. [11], however, did not observe any thermal effect on the samples studied within the same temperature range, though with different precursors. Similarly, the work by Petkov et al. [11] did not show any special features in its heat capacity. Their work and others showed that using different precursors of the starting materials leads to different effects, particularly, the peaks and their positions. The area of the peak in this sample is the smallest, comparatively, showing that the reaction involving the evolution of water released the least amount of heat. In the system  $\text{Li}_{1+x}\text{Ti}_{2-x}\text{Al}_x(\text{PO}_4)_3$  ( $0.5 < x < 0.9$ ), the DTA did not show any structural changes on heating, though melting was observed above 800 °C [12]. Similarly, Oda et al. [13] observed the DTA peaks in a temperature region different from the TG in  $\text{Li}_{1+x}\text{GaTi}_{2-x}(\text{PO}_4)_3$  with  $x = 0.1\text{--}0.9$ . From [www.netl.doe.gov/publications/proceedings/03/ucr-hcbu/Brown/pdf](http://www.netl.doe.gov/publications/proceedings/03/ucr-hcbu/Brown/pdf), accessed, 2009, the authors studied NZP  $x = 0.00$  by sol-gel preparation and obtained similar results, had one exothermic peak in the DTA at 270 °C from 220 to 280 °C, overall mass loss of 29%, RT 1000 °C and with approximately four temperature regions showing stability from 600 °C.

The sample  $x = 0.25$  showed one sharp exothermic peak at 200 °C, starting from 180 to 250 °C which is also ascribed to the loss of water and water of hydration. A

plateau exists from 670 to 760 °C, showing that the stability region for this sample began at an earlier temperature (Fig. 2). This means that the increment of lithium content in the sample has increased the thermal stability of the compound compared to the  $x = 0.00$  sample.

In the case of  $x = 0.50$  sample, there is a sharp exothermic peak at 196.4 °C from 163 to 250 °C, is also attributed to the loss of water of hydration and moisture. A plateau is observed between 580 and 700 °C (Fig. 3) which is wider than the previous samples. There is a broad exothermic peak at about 800 °C which may point to the beginning of crystallization process.

The last sample  $x = 0.75$  showed the largest and broadest exothermic peak at 202.6 °C between 140 and 250 °C, showing the loss of water and water of hydration. Similarly, a plateau at 650–720 °C is observed which is the widest region of stability compared to the others (Fig. 4). This is a confirmation of the fact that increasing lithium content brings about thermal stability of the sample, by decreasing the rate of loss of mass of the sample, as confirmed by the TG results below. Also the positions of the exothermic peaks are shifted towards higher temperatures with increasing lithium contents.

The position of the peaks is shifting with increased lithium content, implying that the lithium increased the thermal stability of the samples, delaying the temperature at which these losses occur. This is confirmed by the TG plot. The TG for all the samples showed the same character and can be approximately broken into four temperature ranges: (1) RT–60 °C, (2) 60–180 °C, (3) 180–360 °C, and (4) 360–1000 °C. In all the samples, 600–1000 °C is the thermal stability region, as the mass loss is about 1% only. The rate of mass loss decreased with increasing temperature through the regions, until it became virtually constant from 600 °C upwards in all the samples. The TG plot is not shown beyond 600 °C because it is virtually constant.

Thus for sample  $x = 0.00$ , the mass loss is 7% in the first region, approximately 5% in the second region, 15% mass in the third, and 2% in the fourth region. The mass loss is greatest in the third and is within the region of the exotherm, as observed in the DTA. Overall, there was a mass loss of about 29% from room temperature to about 1000 °C (Fig. 5). The TG plot shows that the sample is stable from around 600 °C and this is in agreement with that of Naik et al. [10] and the general characteristics of the plots are the same in terms of mass losses in the various regions. This implies that the formation reaction of the product was complete at this temperature. This is also in agreement with the DTA results discussed above for the sample. In their study of  $\text{Li}_{1+x}\text{Ti}_{2-x}\text{Al}_x(\text{PO}_4)_3$  ( $0.5 < x < 0.9$ ), Mouahid et al. [12] did not observe any mass losses in the TG from room temperature up to 800 °C.

In the same region for sample  $x = 0.25$ , the mass losses were 6, 4, 16, and 2.5%, respectively. Similarly, the mass loss is the greatest in the third region, almost the same amount with the  $x = 0.00$  sample. Overall mass loss was approximately 29% (Fig. 6), as in the sample  $x = 0.00$  and correlates with the sample  $x = 0.00$  in terms of the greatest amount of mass loss in the third region. Similarly, the rate of mass loss with changing temperature decreased, showing that the material has become more stable with increase in lithium content.

Similarly, for  $x = 0.50$ , respective mass losses in the regions were 5, 3, 13, and 2% confirming further the activity in the exothermic region, i.e., third region. Again there is a slight decrease in the rate of mass loss with changing temperature compared to the earlier samples. Overall mass loss was 23% (Fig. 7), and further evidence of the comparative stability of this sample.

The last sample,  $x = 0.75$  has, respectively, 2, 2.5, and 5% in the regions with overall mass loss of 25% (Fig. 8). The mass loss has drastically reduced in the third region to only 5% and beyond, showing that the lithium content at this level has dramatically increased the stability of the sample with the rate of mass loss with increased temperature being the lowest. The results show an increasing stability of the samples with increased lithium content.

It is clear that the samples exhibited the same characteristics, with the four temperature domains clearly visible and mass losses occurring at about the same temperature range. Within the temperature range RT–60 °C,  $x = 0.00$  showed the highest mass loss of about 30%, with  $x = 0.75$  being the least. Similarly, between RT and 360 °C, the plots maintained a particular order in terms of mass loss with  $x = 0.75 < 0.50 < 0.25 < 0.00$ . The mass loss decreased with increasing lithium content. Beyond this temperature, the mass loss for the  $x = 0.00 > x = 0.25$  up to about 500 °C, thereafter they maintained virtually the same mass loss. Whereas the  $x = 0.50$  sample became more stable, with less loss in mass than  $x = 0.75$  and beyond 360 °C. The  $x = 0.50$  and 0.25 have the same mass loss from RT to 170 °C, about 5%. The fourth region has the least loss in mass in all the samples and almost the same magnitude. Although Petkov et al. [14] have studied in details the compositions  $\text{Na}_{1-x}\text{Li}_x\text{Zr}_2(\text{PO}_4)_3$ ,  $x = 0.0, 0.50, 0.8$  and 1.00 by TG/DTA and other characterizations, they did not provide the plots for comparison.

## Conclusions

The systematic increase in the lithium content of the samples leads to the compound formation at lower temperature. The exothermic peaks were observed to shift

towards higher temperatures with increased lithium content just as the process itself shifted towards higher temperatures from its lower limits. Consequently, the thermal stability regions become wider with increased lithium content. Work is ongoing to characterize the phase and other properties of the compound before conclusive deductions can be made, though the material has already exhibited the NZP character from the plots.

**Acknowledgements** The authors would like to thank Engineer Shehu Ahmed Isah, of NMDC, Jos, for help with the Furnace work, Mr. A. S. Afolabi of the University of Witwatersrand, South Africa, and Mr. A. Jegede of CERD, OAU, Ife, for thermal characterization. Also we thank Prof. Sunday Thomas, D-G. Shestco, Abuja, and Dr. T. Salkus of Vilnius University, Lithuania, for their various roles in the synthesis of the materials.

## References

1. Dinesh AK, Girish H, Else B, Rustum R. [NZP],  $\text{NaZr}_2\text{P}_3\text{O}_{12}$ -type materials for protection of carbon-carbon composites. *J Mater Res.* 1996;11:3160.
2. Lee WY, Cooley KM, Berndt CC, Joslin DL, Stinton DP. High temperature chemical stability of plasma-sprayed  $\text{Ca}_{0.5}\text{Sr}_{0.5}\text{Zr}_4\text{P}_6\text{O}_{24}$  coatings on nicalon/SiC ceramic matrix composite and Nickel based superalloy substrates. *J Am Ceram Soc.* 1996;79:2759–62.
3. Susumu N, Katsuhito I. Immobilization technique of caesium to  $\text{HZr}_2(\text{PO}_4)_3$  using an autoclave. *J Nucl Sci Technol.* 2003;40: 631–3.
4. Pet'kov VI, Orlova AI. Crystal-chemical approach to predicting the thermal expansion of compounds in the NZP family. *Inorg Mater.* 2003;39:1013–23.
5. Taracson JM, Armand M. Issues and challenges facing lithium batteries. *Nature.* 2001;414:362.
6. Fuentes RO, Lamas DG, Fernandez DE, Rapp ME, Figuiredo FM, Frade JR, et al. Restriction to obtain NASICON by ceramic route. *Boll De la Soc Ceram.* 2004;14:777.
7. Kumar PP, Yashonath Y. Ionic conduction in the solid state. *J Chem Soc.* 2006;118:147.
8. Anantharamulu N, Prasad G, Vithal M. Preparation, characterization and conductivity studies of  $\text{Li}_{3-2x}\text{Al}_{2-x}\text{Sb}_x(\text{PO}_4)_3$ . *Bull Mater Sci.* 2008;31:134.
9. Kang HB, Cho NH. Phase formation, sintering behaviour and electrical characteristics of NASICON compounds. *J Mater Sci.* 1999;34:5006.
10. Naik AH, Thakkar NV, Darwatkar SR, Mudher KDS, Venagopal VV. Microwave assisted low temperature synthesis of sodium zirconium phosphate ( $\text{NaZr}_2(\text{PO}_4)_3$ ). *J Therm Anal Calorim.* 2004;76:707–13.
11. Petkov VI, Asabina EA, Markin AV, Smirnova NN. Synthesis, characterization and thermodynamic data of compounds with NZP structure. *J Therm Anal Calorim.* 2008;91:157–8.
12. Mouahid FE, Zahir M, Maldonado-Manso PM, Bruque S, Losilla ER, Aranda MAG, et al. Na-Li exchange of  $\text{Na}_{1+x}\text{Ti}_{2-x}\text{Al}_x(\text{PO}_4)_3$  ( $0.6 \leq x \leq 0.9$ ) NASICON series: a Rietveld and impedance study. *J Mater Chem.* 2001;11:3258–63.
13. Oda K, Takase S, Shimizu Y. Preparation of high conductive lithium ceramic. *Mater Sci Forum.* 2007;544–545:1033–6.
14. Petkov VI, Orlova AI, Trubach IG, Asabina YA, Demarin VT, Kurazhkovskaya VS. Immobilization of nuclear waste materials containing different alkali elements in single-phase NZP-based ceramics. *Czech J Phys.* 2003;53:A639–48.